Terahertz Spectroscopy of Spin Waves in Multiferroic $BiFeO_3$ in High Magnetic Fields

U. Nagel,[1,*] Randy S. Fishman,[2] T. Katuwal,[1,†] H. Engelkamp,[3] D. Talbayev,[4]
Hee Taek Yi,[5] S.-W. Cheong,[5] and T. Rõõm[1]

[1]*National Institute of Chemical Physics and Biophysics, Akadeemia tee 23, 12618 Tallinn, Estonia*
[2]*Oak Ridge National Laboratory, Materials Science and Technology Division, Oak Ridge, Tennessee 37831, USA*
[3]*High Field Magnet Laboratory, Institute for Molecules and Materials, Radboud University Nijmegen, Toernooiveld 7, 6525 ED Nijmegen, The Netherlands*
[4]*Department of Physics, Tulane University, 5032 Percival Stern Hall, New Orleans, Louisiana 70118, USA*
[5]*Rutgers Center for Emergent Materials and Department of Physics and Astronomy, Rutgers University, 136 Frelinghuysen Road, Piscataway, New Jersey 08854, USA*

(Received 12 February 2013; revised manuscript received 17 May 2013; published 17 June 2013)

We have studied the magnetic field dependence of far-infrared active magnetic modes in a single ferroelectric domain $BiFeO_3$ crystal at low temperature. The modes soften close to the critical field of 18.8 T along the [001] (pseudocubic) axis, where the cycloidal structure changes to the homogeneous canted antiferromagnetic state and a new strong mode with linear field dependence appears that persists at least up to 31 T. A microscopic model that includes two Dzyaloshinskii-Moriya interactions and easy-axis anisotropy describes closely both the zero-field spectroscopic modes as well as their splitting and evolution in a magnetic field. The good agreement of theory with experiment suggests that the proposed model provides the foundation for future technological applications of this multiferroic material.

DOI: 10.1103/PhysRevLett.110.257201 PACS numbers: 75.85.+t, 76.50.+g, 78.30.−j

Because of the coupling between electric and magnetic properties, multiferroic materials are among the most important yet discovered. With a multiferroic material used as a storage medium, information can be written electrically and then read magnetically without Joule heating [1]. Hence, applications of a room-temperature multiferroic would radically transform the magnetic storage industry. Because it is the only known room-temperature multiferroic, $BiFeO_3$ continues to attract intense interest.

Although its ferroelectric transition temperature [2] $T_c \approx 1100$ K is much higher than its Néel transition temperature [3–5] $T_N \approx 640$ K, the appearance of a long-wavelength cycloid [3,6–8] with a period of 62 nm enhances the ferroelectric polarization below T_N. The induced polarization has been used to switch between magnetic domains with an applied electric field [4,5,9].

Progress in understanding the microscopic interactions in $BiFeO_3$ has been greatly accelerated by the recent availability of single crystals for both elastic and inelastic neutron-scattering measurements. By fitting the spin wave frequencies above a few meV, recent measurements [10,11] have determined the antiferromagnetic (AFM) nearest-neighbor and next-nearest-neighbor exchanges $J_1 \approx -4.5$ meV and $J_2 = -0.2$ meV. In the presence of strain [12], nonmagnetic impurities [13], or a magnetic field [14,15] above $B_c \approx 19$ T, those exchange interactions produce a G-type antiferromagnet with ferromagnetic alignment of the $S = 5/2$ Fe^{3+} spins within each hexagonal plane, (111) in cubic notation.

Below B_c, the magnetic order in $BiFeO_3$ is created by the much smaller anisotropy and Dzyaloshinskii-Moriya interactions. Neutron scattering is typically used to determine the weak interactions that produce a complex spin state. Because the wavelength $a/\sqrt{2}\delta$ of $BiFeO_3$ is so large, however, inelastic neutron-scattering measurements cannot resolve the cycloid satellite peaks at $\mathbf{q} = (2\pi/a) \times (0.5 \pm \delta, 0.5, 0.5 \mp \delta)$, on either side of the AFM wave vector $\mathbf{Q}_0 = (\pi/a)(1, 1, 1)$, where $a \approx 3.96$ Å is the pseudocubic lattice constant. Below 5 meV, inelastic measurements at $\mathbf{q}_0$ reveal four broad peaks, each of which can be roughly assigned to one or more of the spin wave branches averaged over the first Brillouin zone [11,16]. By contrast, terahertz spectroscopy [17,18] provides very precise measurements for the optically active spin wave frequencies at the cycloid wave vector $\mathbf{q}$.

Symmetry allows three possible directions of the cycloidal ordering vector $\mathbf{q}_k \parallel \{[1, \bar{1}, 0], [0, 1, \bar{1}], [\bar{1}, 0, 1]\} \perp \mathbf{P}$ (see Fig. 1). The spins of a cycloid $\mathbf{q}_k$ are in the plane determined by $\mathbf{P}$ and $\mathbf{q}_k$. The cycloidal order in $BiFeO_3$ is induced by a weak Dzyaloshinskii-Moriya interaction that couples spins along $\mathbf{q}_k$ with coupling $\mathbf{D} \perp \mathbf{P}$ and $\mathbf{D} \perp \mathbf{q}_k$ [19]. Another Dzyaloshinskii-Moriya-like interaction $\mathbf{D}' \parallel \mathbf{P} \parallel [111]$ couples spins on the [111] direction. It is induced by magnetoelectric coupling and cants spins out of the cycloid plane [19–21]. The ferromagnetic ordering of this canted moment has been verified by a neutron scattering experiment [22]. High resolution neutron scattering shows that the magnetic ground state ordering in $BiFeO_3$ does not change in zero field on cooling from 300 to 4 K [6,23,24].

Single ion anisotropy K along the easy axis [111] introduces anharmonicity [19,25], but in zero magnetic field the cycloid is only slightly anharmonic [6,8]. An external

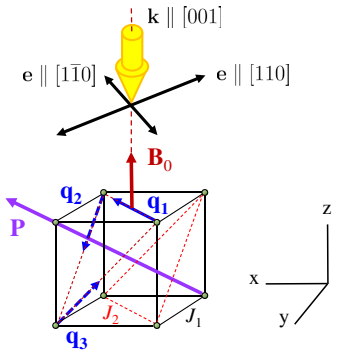

FIG. 1 (color online). Pseudocubic unit cell of $BiFeO_3$ showing the positions of Fe ions, the ferroelectric polarization $\mathbf{P}$, three equivalent directions of the cycloidal ordering vector $\mathbf{q}_k$, the applied static magnetic field $\mathbf{B}_0 \parallel [001]$, and the wave vector of incident light $\mathbf{k}$ together with the electric field ($\mathbf{e}$) component of light in two orthogonal polarizations that were used in the experiment. J_1 and J_2 are the nearest- and next-nearest-neighbor exchange interactions.

magnetic field contributes to the effective single ion anisotropy [26] and induces a metamagnetic transition [19] at the critical field $B_c \approx 19$ T, where the cycloidal order changes to a collinear AFM spin order [27]. The unwinding of the cycloid reduces the electric polarization [15] and creates a small macroscopic spontaneous magnetization induced by $\mathbf{D}' \parallel [111]$ [15,19].

The frequencies of magnetic modes are sensitive to anisotropic magnetic interactions and these interactions are important to understand the microscopic models behind the magnetoelectric coupling in multiferroics. The eigenspectrum of $BiFeO_3$ cycloids was calculated by de Sousa and Moore [28], with the addition of single-ion easy-axis anisotropy by Fishman *et al.* [16,29] in 0 T and in an applied electric field by Rovillain *et al.* [30]. Spectroscopic techniques that measure the eigenspectrum of magnetic modes are valuable tools, especially if they can be combined with external fields that compete with internal fields. The Raman work demonstrated that the Raman-active spin wave frequencies depend strongly on the applied electric field [30]. Most of the INS [10,11], Raman [31,32], and terahertz [17,33] spectroscopy studies on $BiFeO_3$ were in zero applied field. The high field ESR was done in magnetic fields up to 25 T, but was limited to frequencies lower than the main cycloid modes and one of the AFM modes.

In this Letter, we present terahertz absorption spectra of a $BiFeO_3$ single crystal at low temperature and follow the magnetic field dependence of cycloid excitations until the cycloidal order is destroyed in the high magnetic field and replaced by a canted AFM order. We show that the proposed microscopic model in addition to describing the frequencies of the cycloid in zero field also predicts the splitting and evolution of the spin wave modes with the magnetic field [16,29]. Due to mode mixing, all of the spin wave modes become optically active in the magnetic field. The close agreement between predictions and measurements suggests that the proposed model can provide the foundation for future work on $BiFeO_3$.

In a magnetic field $\mathbf{H} = H\mathbf{m}$ along $\mathbf{m}$, the spin state and spin wave excitations of $BiFeO_3$ are evaluated from the Hamiltonian

$$\begin{aligned}\mathcal{H} = & -J_1 \sum_{\langle i,j \rangle} \mathbf{S}_i \cdot \mathbf{S}_j - J_2 \sum_{\langle i,j \rangle'} \mathbf{S}_i \cdot \mathbf{S}_j - K \sum_i (\mathbf{S}_i \cdot \mathbf{z}')^2 \\ & - D \sum_{\mathbf{R}_j = \mathbf{R}_i + a(\mathbf{x}-\mathbf{z})} \mathbf{y}' \cdot (\mathbf{S}_i \times \mathbf{S}_j) \\ & - D' \sum_{\mathbf{R}_j = \mathbf{R}_i + a\mathbf{x}, a\mathbf{y}, a\mathbf{z}} (-1)^{R_{iz'}/c} \mathbf{z}' \cdot (\mathbf{S}_i \times \mathbf{S}_j) \\ & - 2\mu_B H \sum_i \mathbf{S}_i \cdot \mathbf{m}. \end{aligned} \quad (1)$$

Here $\mathbf{z}' \parallel [1,1,1]$, $\mathbf{x}' \parallel \mathbf{q}_k$, and $\mathbf{y}' = \mathbf{z}' \times \mathbf{x}'$, where $k = 1$, 2, 3 are the indexes of the three cycloids that are symmetry equivalent in zero field and $c = a/\sqrt{3}$ is the distance between neighboring (1, 1, 1) planes. While the nearest- and next-nearest-neighbor exchange interactions $J_1 = -4.5$ meV and $J_2 = -0.2$ meV can be obtained from the spin wave dispersion between 5.5 and 72 meV [10,11] the small interactions $D = 0.107$ meV, $D' = 0.054$ meV, and $K = 0.0035$ meV that control the cycloid [29] are obtained from the terahertz spectra below 5.5 meV (44.3 cm^{-1}), measured in zero magnetic field. For a given set of interaction parameters and magnetic field, the spin state of $BiFeO_3$ is obtained by minimizing the energy $E = \langle \mathcal{H} \rangle$.

The (001) face single crystal $BiFeO_3$ sample was grown using a Bi_2O_3 flux [34]. It has a thickness of 0.37 mm and it contains a single ferroelectric domain, $\mathbf{P} \parallel [111]$ axis in Fig. 1, checked by an optical rectification experiment [35].

The sample was zero field cooled and spectra were measured in the Faraday configuration with the magnetic field along the [001] axis. Up to 12 T spectra were measured at 4 K in Tallinn with a SPS-200 Martin-Puplett spectrometer from Sciencetech Inc. and a 0.3 K bolometer [36] using a spectral resolution of 0.2 cm^{-1}. Spectra from 12 up to 31 T were measured in the Nijmegen High Field Magnet Laboratory at 2 K using a Bruker IFS 113v spectrometer and a 1.6 K silicon bolometer and a spectral resolution of 0.43 cm^{-1}; the spectra were averaged for 15 min at each field. There was a linear polarizer in front of the sample to control the polarization of light.

We measured absorbance spectra in the magnetic field with the reference spectrum in zero field. This method gave excellent spectra of the magnetic field dependent lines. From the differential absorbance spectra in fields above 21 T (after applying 30 T) we extracted the zero field absorption lines, solid curves in Fig. 2, and fitted them. The fit results were added to the measured differential spectra in the magnetic fields. The result, absolute absorbance spectra in the fields, is shown in the Supplemental Material [37] and the fitted line positions and areas are shown in Fig. 3.

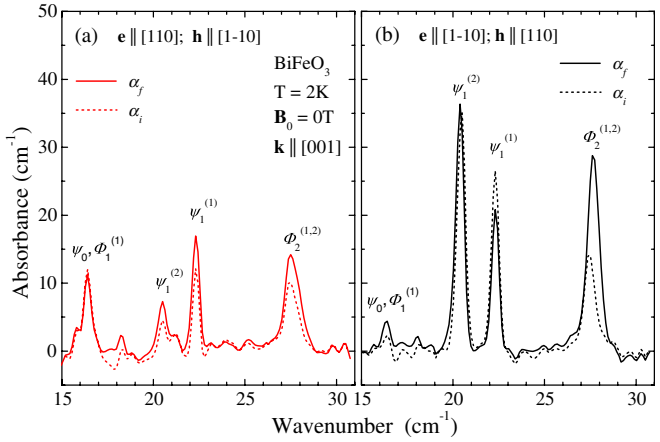

FIG. 2 (color online). Absorbance spectra of spin wave modes in zero field in $\mathbf{e} \parallel [110]$ polarization (a) and in $\mathbf{e} \parallel [1\bar{1}0]$ polarization (b). Solid curves α_F were measured after applying the high field $\mathbf{B}_0 \geq 21$ T. Dotted curves are initial absorbance spectra α_I of the zero field cooled sample.

A change in the zero field spectra was observed after applying the high field at low temperature (see Fig. 2). The zero field spectrum stayed the same after applying the high field again or in the opposite direction. The initial zero field line intensities α_I, measured on the zero field cooled sample, were recovered after warming the sample to 300 K. This is evidence that different magnetic domains exist. We found that the change in the zero field spectra, as measured after applying magnetic fields at low temperature, occurs already by 12 T and higher fields that destroy the cycloid do not change the zero field lines any more (see the Supplemental Material [37]). The calculation shows that for $\mathbf{B}_0 \parallel [001]$ the $\mathbf{q}_1$ cycloid where the field is mostly perpendicular to the cycloid plane has a lower energy than cycloids $\mathbf{q}_2$ and $\mathbf{q}_3$ (see the Supplemental Material [37]). However, some fraction of $\mathbf{q}_2$ and $\mathbf{q}_3$ domains follow the magnetic field without hysteresis below 5 T as discussed below. This suggests that crystal imperfections act as a barrier to maintain the dominant $\mathbf{q}_1$ domain after the field has been removed. Clearly there is a thermally activated hysteresis, but in this study we concentrate on the low temperature spectra that are measured after the sample had been in the high field ≥ 12 T.

The detailed field dependence of mode frequencies and areas is presented in Fig. 3. The three main modes, $\Psi_1^{(2)}$, $\Psi_1^{(1)}$, and $\Phi_2^{(1,2)}$ change only slightly with increasing magnetic field until about 5 T is reached, where a discontinuity of several mode frequencies and a smooth change in the slope of the $\Psi_1^{(2)}$ mode is observed. These changes are associated with the change in the magnetic domain structure, where modes of the q_2 and q_3 domains (blue dotted lines) are depopulated and only the modes of the q_1 domain (blue solid lines) remain observable in higher fields. To reflect this behavior we have cut off the predicted mode frequencies of domains q_2 and q_3 above 6 T.

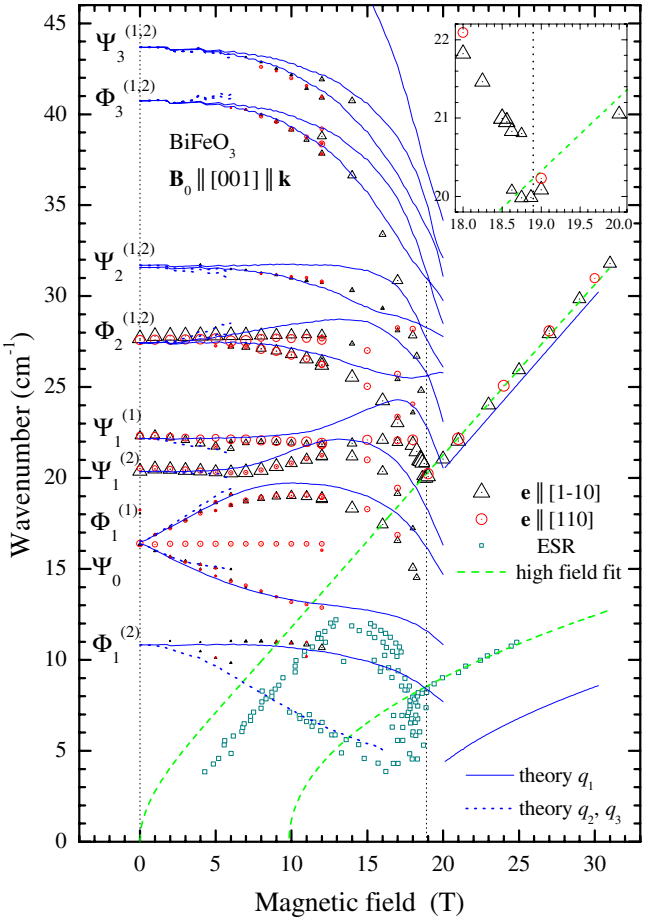

FIG. 3 (color online). Magnetic field dependence of spin wave modes in the terahertz absorption spectrum of $BiFeO_3$ at low temperature. The areas of triangles and circles are proportional to the absorption line areas. The vertical dashed line at $B_c = 18.8$ T marks the metamagnetic transition. Green dashed lines are the fit of our data and ESR data [38] (squares) above 19 T to a model from Ref. [38]. Blue solid lines are calculated modes of cycloid q_1. Dotted blue lines are calculated modes of cycloids q_2 and q_3, shown only below 6 T where corresponding excitations are observed in measured spectra; the lowest energy mode is shown also for higher fields since there is a matching excitation in ESR data. The theoretically predicted metamagnetic transition is at 20 T for cycloid $\mathbf{q}_1$ and at 16.5 T for cycloids $\mathbf{q}_2$ and $\mathbf{q}_3$.

The modes soften before reaching the metamagnetic transition at B_c, except for $\Psi_1^{(1)}$ which seems to merge with the softening $\Phi_2^{(1,2)}$ at about 18 T. There is an intriguing possibility that close to the transition between 18.6 and 18.8 T (see the inset to Fig. 3) one of the cycloid resonances $\Psi_1^{(1)}$ or $\Phi_2^{(1,2)}$ as labeled in zero field coexists with the AFM resonance. This means that in a narrow field interval the spin structure supports both cycloidal and AFM modes. The coexistence of two phases is ruled out since the metamagnetic transition in $BiFeO_3$ is neither the first order phase transition nor similar to a spin flop transition in ordinary antiferromagnets [26] and also we did not observe

any hysteresis effects between 18 and 19 T as reported earlier [38]. In terahertz spectra there is only one resonance line above 18.8 T and we assign this value to the critical field B_c of the metamagnetic transition in $BiFeO_3$ at 2 K and $\mathbf{B}_0 \parallel [001]$. However, the terahertz spectra do not show any anomalies at 10 T seen by optical measurements [39].

The AFM resonances in $BiFeO_3$ can also be described by a phenomenological theory [38] and we use it to fit the ESR [38] and terahertz data in the homogeneous canted antiferromagnetic state (see the dashed lines in Fig. 3). The fit gives the following parameters: gyromagnetic ratio $\gamma = (1.72 \pm 0.01) \times 10^7$ rad(s Oe)$^{-1}$, $K_u/\chi_\perp = (1.06 \pm 0.02) \times 10^{10}$ erg cm^{-3}, $H_{\mathrm{DM}} = (105 \pm 2)$ kOe. K_u is the energy density of the uniaxial magnetic anisotropy and $\chi_\perp$ is the susceptibility perpendicular to the AFM vector, the difference of magnetizations of two sublattices of a G-type antiferromagnet. H_{DM} is the Dzyaloshinskii-Moriya field associated with $\mathbf{D}'$.

We get $K_u = 6.2 \times 10^5$ erg cm^{-3} using $\chi_\perp = 5.8 \times 10^{-5}$ from the high field magnetization measurement [14]. The value we get for the same quantity from our microscopic theory is $\langle KS_z^2 \rangle = 5.6 \times 10^5$ erg cm^{-3}, where $K = 0.0035$ meV and $S_z = 5/2$. The canted moment as estimated from the AFM resonance spectra $\chi_\perp H_{\mathrm{DM}} = 0.041 \mu_B$/Fe should be compared to $0.03 \mu_B$ derived from the extrapolation of the high field magnetization to the zero field [14]. Thus, the parameters derived from the phenomenological model are very close to the values used in the microscopic theory.

Considering the microscopic theory, the agreement between the measured and predicted mode frequencies in Fig. 3 is remarkable. In agreement with predictions, Ψ_0 and $\Phi_1^{(1)}$ are slightly lower in domain q_1 than in domains q_2 and q_3. The predicted splitting of $\Phi_2^{(1,2)}$ is clearly seen in Fig. 3. Also in agreement with predictions, $\Psi_1^{(1)}$ is slightly lower in domains q_2 and q_3 than in domain q_1. The only feature that remains unexplained by our model is the field-independent mode observed at about 16.5 cm^{-1}, midway between $\Phi_1^{(1)}$ and Ψ_0 which becomes too weak to be detected in the Nijmegen setup and thus cannot be followed until it disappears at $\mathbf{B}_c = 18.8$ T. Notice that several modes in Fig. 3 only become optically active in the magnetic field. Recall that in our microscopic model we use the same interaction parameters that were previously obtained for zero field [29]. Therefore, it is not surprising that the quantitative agreement with measurements, although quite good, is not perfect. In particular, the lower frequency AFM mode in the canted phase is predicted to be about 4 cm^{-1} lower than that measured by ESR.

To conclude, the close agreement between the predicted and observed spin wave frequencies in the magnetic field leaves no doubt about the origin of those modes. This agreement suggests that the present model, with Dzyaloshinskii-Moriya interactions along $\mathbf{y}'$ and $\mathbf{z}'$ and easy-axis anisotropy along $\mathbf{z}'$, can provide the foundation for future studies on $BiFeO_3$ and may lay the groundwork for its eventual technological applications. Our work demonstrates that in addition to an electric field [5], the control of magnetic domains with a magnetic field is possible.

We acknowledge conversations with Nobuo Furukawa, Masaaki Matsuda, Shin Miyahara, Satoshi Okamoto, and Rogerio de Sousa. We acknowledge support by the Estonian Ministry of Education and Research Grant No. SF0690029s09, Estonian Science Foundation Grants No. ETF8170, No. ETF8703, and No. ERMOS67, and by EuroMagNET under the EU Contract No. 228043. Work at Rutgers was supported by DOE Grant No. DE-FG02-07ER46382. R. S. F acknowledges support by the U.S. Department of Energy, Office of Basic Energy Sciences, Materials Sciences and Engineering Division.

*urmas.nagel@kbfi.ee
†On leave from Department of Physics, Trichandra College, Tribhuvan University, Kathmandu, Nepal.

[1] W. Eerenstein, N. D. Mathur, and J. F. Scott, Nature (London) **442**, 759 (2006).
[2] J. R. Teague, R. Gerson, and W. J. James, Solid State Commun. **8**, 1073 (1970).
[3] I. Sosnowska, T. Peterlin-Neumaier, and E. Steichele, J. Phys. C **15**, 4835 (1982).
[4] D. Lebeugle, D. Colson, A. Forget, M. Viret, A. M. Bataille, and A. Goukasov, Phys. Rev. Lett. **100**, 227602 (2008).
[5] S. Lee, W. Ratcliff, S.-W. Cheong, and V. Kiryukhin, Appl. Phys. Lett. **92**, 192906 (2008).
[6] M. Ramazanoglu, W. Ratcliff, Y. J. Choi, S. Lee, S.-W. Cheong, and V. Kiryukhin, Phys. Rev. B **83**, 174434 (2011).
[7] J. Herrero-Albillos, G. Catalan, J. A. Rodriguez-Velamazan, M. Viret, D. Colson, and J. F. Scott, J. Phys. Condens. Matter **22**, 256001 (2010).
[8] I. Sosnowska and R. Przeniosło, Phys. Rev. B **84**, 144404 (2011).
[9] S. Lee, T. Choi, W. Ratcliff, R. Erwin, S.-W. Cheong, and V. Kiryukhin, Phys. Rev. B **78**, 100101 (2008).
[10] J. Jeong, E. A. Goremychkin, T. Guidi, K. Nakajima, G. S. Jeon, S.-A. Kim, S. Furukawa, Y. B. Kim, S. Lee, V. Kiryukhin, S.-W. Cheong, and J.-G. Park, Phys. Rev. Lett. **108**, 077202 (2012).
[11] M. Matsuda, R. S. Fishman, T. Hong, C. H. Lee, T. Ushiyama, Y. Yanagisawa, Y. Tomioka, and T. Ito, Phys. Rev. Lett. **109**, 067205 (2012).
[12] F. Bai, J. Wang, M. Wuttig, J. Li, N. Wang, A. P. Pyatakov, A. K. Zvezdin, L. E. Cross, and D. Viehland, Appl. Phys. Lett. **86**, 032511 (2005).
[13] P. Chen, O. Gunaydin-Sen, W. J. Ren, Z. Qin, T. V. Brinzari, S. McGill, S.-W. Cheong, and J. L. Musfeldt, Phys. Rev. B **86**, 014407 (2012).
[14] M. Tokunaga, M. Azuma, and Y. Shimakawa, J. Phys. Soc. Jpn. **79**, 064713 (2010).
[15] J. Park, S.-H. Lee, S. Lee, F. Gozzo, H. Kimura, Y. Noda, Y. J. Choi, V. Kiryukhin, S.-W. Cheong, Y. Jo, E. S. Choi,

L. Balicas, G. S. Jeon, and J.-G. Park, J. Phys. Soc. Jpn. **80**, 114714 (2011).
[16] R. S. Fishman, N. Furukawa, J. T. Haraldsen, M. Matsuda, and S. Miyahara, Phys. Rev. B **86**, 220402 (2012).
[17] D. Talbayev, S. A. Trugman, S. Lee, H. T. Yi, S.-W. Cheong, and A. J. Taylor, Phys. Rev. B **83**, 094403 (2011).
[18] D. Hüvonen, U. Nagel, T. Rõõm, Y. J. Choi, C. L. Zhang, S. Park, and S.-W. Cheong, Phys. Rev. B **80**, 100402 (2009).
[19] A. M. Kadomtseva, A. K. Zvezdin, Y. P. Popov, A. P. Pyatakov, and G. P. Vorobev, JETP Lett. **79**, 571 (2004).
[20] C. Ederer and N. A. Spaldin, Phys. Rev. B **71**, 060401 (2005).
[21] D. Albrecht, S. Lisenkov, W. Ren, D. Rahmedov, I. A. Kornev, and L. Bellaiche, Phys. Rev. B **81**, 140401 (2010).
[22] M. Ramazanoglu, M. Laver, W. Ratcliff, S. M. Watson, W. C. Chen, A. Jackson, K. Kothapalli, S. Lee, S.-W. Cheong, and V. Kiryukhin, Phys. Rev. Lett. **107**, 207206 (2011).
[23] R. Przeniosło, A. Palewicz, M. Regulski, I. Sosnowska, R. M. Ibberson, and K. S. Knight, J. Phys. Condens. Matter **18**, 2069 (2006).
[24] J. Herrero-Albillos, G. Catalan, J. A. Rodriguez-Velamazan, M. Viret, D. Colson, and J. F. Scott, J. Phys. Condens. Matter **22**, 256001 (2010).
[25] A. M. Kadomtseva, Y. P. Popov, A. P. Pyatakov, G. P. Vorob'ev, A. K. Zvezdin, and D. Viehland, Phase Transit. **79**, 1019 (2006).
[26] M.-M. Tehranchi, N. F. Kubrakov, and A. K. Zvezdin, Ferroelectrics **204**, 181 (1997).
[27] K. Ohoyama, S. Lee, S. Yoshii, Y. Narumi, T. Morioka, H. Nojiri, G. S. Jeon, S.-W. Cheong, and J.-G. Park, J. Phys. Soc. Jpn. **80**, 125001 (2011).
[28] R. de Sousa and J. E. Moore, Phys. Rev. B **77**, 012406 (2008).
[29] R. S. Fishman, J. T. Haraldsen, N. Furukawa, and S. Miyahara, Phys. Rev. B **87**, 134416 (2013).
[30] P. Rovillain, R. de Sousa, Y. Gallais, A. Sacuto, M. A. Méasson, D. Colson, A. Forget, M. M. Bibes, A. Barthélémy, and M. Cazayous, Nat. Mater. **9**, 975 (2010).
[31] M. Cazayous, Y. Gallais, A. Sacuto, R. de Sousa, D. Lebeugle, and D. Colson, Phys. Rev. Lett. **101**, 037601 (2008).
[32] P. Rovillain, M. Cazayous, Y. Gallais, A. Sacuto, R. P. S. M. Lobo, D. Lebeugle, and D. Colson, Phys. Rev. B **79**, 180411 (2009).
[33] G. A. Komandin, V. I. Torgashev, A. A. Volkov, O. E. Porodinkov, I. E. Spektor, and A. A. Bush, Phys. Solid State **52**, 734 (2010).
[34] T. Choi, S. Lee, Y. J. Choi, V. Kiryukhin, and S.-W. Cheong, Science **324**, 63 (2009).
[35] D. Talbayev, A. D. LaForge, S. A. Trugman, N. Hur, A. J. Taylor, R. D. Averitt, and D. N. Basov, Phys. Rev. Lett. **101**, 247601 (2008).
[36] T. Rõõm, D. Hüvonen, U. Nagel, Y.-J. Wang, and R. K. Kremer, Phys. Rev. B **69**, 144410 (2004).
[37] See Supplemental Material at http://link.aps.org/supplemental/10.1103/PhysRevLett.110.257201 for table with fit results of absorption lines in zero magnetic field, and figures showing the absorption spectra in selected magnetic fields, and the calculated energy per site of cycloids in the magnetic field along [001] direction.
[38] B. Ruette, S. Zvyagin, A. P. Pyatakov, A. Bush, J. F. Li, V. I. Belotelov, A. K. Zvezdin, and D. Viehland, Phys. Rev. B **69**, 064114 (2004).
[39] X. S. Xu, T. V. Brinzari, S. Lee, Y. H. Chu, L. W. Martin, A. Kumar, S. McGill, R. C. Rai, R. Ramesh, V. Gopalan, S. W. Cheong, and J. L. Musfeldt, Phys. Rev. B **79**, 134425 (2009).